

Randomized and Inner-product Free Krylov Methods for Large-scale Inverse Problems

Malena Sabaté Landman¹, Ariana N. Brown², Julianne Chung³,
James G. Nagy^{4*}

¹Mathematical Institute, University of Oxford, Oxford, OX2 6GG, UK.

²Dept. of Mathematics, Emory University, Atlanta, 30322, GA, USA.

³Dep. of Mathematics, Emory University, Atlanta, 30322, GA, USA.

⁴Dep. of Mathematics, Emory University, Atlanta, 30322, GA, USA.

*Corresponding author(s). E-mail(s): jnagy@emory.edu;

Contributing authors: Malena.SabateLandman@maths.ox.ac.uk;

ariana.brown@emory.edu; jmchung@emory.edu;

Abstract

Iterative Krylov projection methods have become widely used for solving large-scale linear inverse problems. However, methods based on orthogonality include the computation of inner-products, which become costly when the number of iterations is high; are a bottleneck for parallelization; and can cause the algorithms to break down in low precision due to information loss in the projections. Recent works on inner-product free Krylov iterative algorithms alleviate these concerns, but they are quasi-minimal residual rather than minimal residual methods. This is a potential concern for inverse problems where the residual norm provides critical information from the observations via the likelihood function, and we do not have any way of controlling how close the quasi-norm is from the norm we want to minimize. In this work, we introduce a new Krylov method that is both inner-product-free and minimizes a functional that is theoretically closer to the residual norm. The proposed scheme combines an inner-product free Hessenberg projection approach for generating a solution subspace with a randomized sketch-and-solve approach for solving the resulting strongly overdetermined projected least-squares problem. Numerical results show that the proposed algorithm can solve large-scale inverse problems efficiently and without requiring inner-products.

Keywords: Krylov methods, least-squares, inverse problems, sketching, randomized

1 Introduction

Inverse problems arise in many different applications including medical and geophysical imaging, electromagnetic scattering, machine learning, and image deblurring [1–4]. Typically, the goal of an inverse problem is to estimate some unknown quantities or parameters of a system, given observations or indirect measurements (e.g., taken on the exterior of the object). In particular, we consider linear discrete inverse problems of the form,

$$b = Ax_{\text{true}} + e, \quad (1)$$

where $A \in \mathbb{R}^{m \times n}$ models the forward problem, $x_{\text{true}} \in \mathbb{R}^n$ is the unknown solution we want to approximate, $b \in \mathbb{R}^m$ is the vector of observed data, and $e \in \mathbb{R}^m$ represents noise and other measurement errors. Given b and A , the goal is to estimate x_{true} , but there are various computational challenges.

For many applications, the number of unknowns n may be very large and the forward model matrix A (and its adjoint) can only be accessed via matrix-vector multiplications. Thus, iterative methods are often used to compute approximations of x_{true} . Moreover, these inverse problems are usually ill-posed in the sense that small perturbations in the observation can cause large perturbations in the computed solution. This is due to the fact that the singular values of A decay and cluster at zero without a gap between consecutive values, and because the singular vectors corresponding to small singular values tend to be highly oscillatory. Indeed, the noiseless right-hand side Ax_{true} satisfies the discrete Picard condition [2], while the noise is captured mostly in the singular subspace associated to the small singular values. Moreover, due to the presence of noise in the measurements, b might not be in the range of A . Regularization can be used to address ill-posedness and can take many forms. In iterative regularization, standard iterative solvers (e.g., Krylov methods) are applied to the least squares problem,

$$\min_{x \in \mathbb{R}^n} \|Ax - b\|_2, \quad (2)$$

and regularization is obtained by early stopping. Variational regularization is another form of regularization, where prior knowledge about the solution properties (e.g., smoothness or sparsity) is included in the regularization term. We focus on standard Tikhonov regularization,

$$\min_{x \in \mathbb{R}^n} \|Ax - b\|_2^2 + \lambda \|x\|_2^2, \quad (3)$$

where $\lambda > 0$ is a regularization parameter that balances the effect of the regularization against the fitting of the data to the noisy measurements (i.e., the likelihood function).

There exists a myriad of iterative methods to solve minimization problems (2) and (3) efficiently. However, the capacity we have to measure and store data is constantly increasing, pushing the limits of traditional least-squares solvers in terms of speed and memory requirements. Recently, different directions have emerged to tackle more challenging scenarios. Some (partial) solutions are motivated in large part by the evolution of commercial hardware. For example, new methods are being investigated that can exploit low precision or mixed precision arithmetic. In particular, these approaches use lower precision for storage and computation and benefit from distributed memory implementations. New methods are being developed that can reduce global communication points, such as the computation of inner products. In another line of

research, randomized numerical linear algebra has emerged as a powerful framework to drastically reduce computational costs. Although initial randomized approaches that were based on obtaining low-rank approximations are not suitable for practical large-scale inverse problems, iterative methods that can exploit randomization for solving least-squares problems are being widely adopted and investigated.

Inner-product-free Krylov subspace methods have recently emerged as competitive alternatives to well-known algorithms for inverse problems. In particular, the changing minimum residual Hessenberg (CMRH) method is a Krylov subspace method similar to generalized minimum residual (GMRES), but instead of using the Arnoldi scheme (in the case of GMRES) to construct an orthonormal basis of the Krylov subspace, CMRH uses a Hessenberg method to construct a good (although not orthonormal) linearly independent basis. Although the Hessenberg method was mentioned in the literature as early as 1950 (see, e.g., [5, section 44]) for computing eigenvalues, it was Sadok [6] who introduced the CMRH method in 1999 as a way to solve linear systems. In 2012, Sadok and Szyld [7] investigated the relationship between CMRH and GMRES. More recently, it was shown that CMRH is a regularizing iterative method, and that further regularization can be incorporated with a hybrid approach, called HCMRH [8]. An extension to rectangular systems, called LSLU was developed in [9] that uses a generalized Hessenberg iterative algorithm to generate linearly independent bases for Krylov subspaces associated with $A^T A$ and AA^T . The approach has a theoretical connection to the LU factorization (with partial pivoting), and the iterative regularization properties of LSLU are very similar to LSQR [10, 11]. The main benefit of LSLU is that no inner-products are required during the iterations (note that we assume that matrix-vector multiplications with A and A^T can be performed via function evaluations). This leads to projected quasi-minimum residual problems that are smaller and easier to solve at each iteration.

In general, a quasi-minimum residual method can provide suitable solutions and various relationships can be made between iterates [12]. However, in the context of inverse problems, the residual norm provides important information regarding the fit-to-data term, which depends on statistical assumptions about the measurement noise. In particular, the solution to LS problem (2) corresponds to a maximum likelihood estimate and the solution to Tikhonov problem (3) corresponds to a maximum a posteriori estimate [13]. Thus, we seek inner-product free Krylov methods that are also minimum residual methods. Unfortunately, this means that a tall, skinny least-squares problem needs to be solved at each iteration. We address this computational challenge by exploiting recent work on randomized methods, which produces solutions that can approximate closely the minimal residual norm at each iteration.

Main Contributions

We propose a new family of Krylov subspace methods that are inherently inner-product free and produce solutions with a smaller residual norm than existing inner-product free Krylov subspace methods. These are based on a (generalized) Hessenberg method with partial pivoting, where either one or two sets of linearly independent vectors are constructed to span Krylov subspaces. Contrary to standard iterative methods, the new approach avoids reorthogonalization and does not require

inner-products. Contrary to other inner-product free Krylov methods, we use randomized sketching to obtain a more accurate approximation of the objective function to be minimized: the norm of the projection of either the residual or the Tikhonov objective function in a Krylov subspace of increasing dimension. The potential implications of this for inverse problems is that for existing inner-product free Krylov methods, it may be challenging to select regularization parameters in a hybrid approach and the bounds for the residuals depend on the conditioning of the basis vectors.

Paper structure

The paper is organized as follows. In Section 2 we give an overview of sketch-and-solve methods for least-squares problems, including choices of sketching matrices. In Section 3, we recall the Hessenberg method to build a linearly independent basis for different choices of Krylov subspaces without requiring inner-products. We present new inner-product free Krylov methods, sketched CMRH (sCMRH) and sketched LSLU (sLSLU), to solve the least-squares problem and introduce an adaptation that considers Tikhonov regularization. Finally, in Section 4, we illustrate the effectiveness of sCMRH and sLSLU, compared to existing iterative methods, and of sLSLU with Tikhonov regularization using a fixed regularization parameter. We provide closing remarks in Section 5

2 Background on randomized methods for least-squares problems

In Section 3.2 we use randomized methods to efficiently solve strongly overdetermined projected LS problems, so the aim of this section is to give some background on randomized methods. Randomized numerical linear algebra, particularly those approaches involving sketching, has gained increasing popularity, see e.g [14]. Sketching is a linear dimensionality reduction technique, and there are different ways in which sketching has been used to solve least squares problems. One of the conceptually simplest approaches is to sketch-and-solve, which can be used to find approximate solutions of least-squares problems where the system matrix is tall and skinny. This was originally proposed in [15] and has gained a lot of attention due to its simplicity and probabilistic guarantees. In particular, we can define a sketching matrix $S \in \mathbb{R}^{\ell \times m}$, such that the following subspace (oblivious) embedding property is satisfied for any vector $a \in \mathbb{R}^m$ in a given set of vectors

$$(1 - \epsilon)\|a\| \leq \|Sa\| \leq (1 + \epsilon)\|a\|. \quad (4)$$

For this to be a dimensionality reduction technique, we typically assume that $\ell \ll m$. Even if this is a very favorable property, it is not trivial to construct such matrices deterministically in practice, in the sense that (4) is guaranteed for any $a \in \mathbb{R}^m$. However, the analytical properties of random matrices can be used to construct sketching matrices $S \in \mathbb{R}^{\ell \times m}$ that will satisfy (4) with high probability. Note that this is a special case of a random subspace embedding; for a formal definition, see, e.g. [14, Chapter 8.1].

Moreover, there exist different choices of random matrices in the literature that can be computationally cheap to construct and apply. In particular, we only consider the embedding of oblivious subspaces, which do not assume any prior information about the set of possible vectors a . The easiest class to analyze and implement is that of Gaussian embeddings, where each entry of $S \in \mathbb{R}^{\ell \times m}$ is an independent draw of a Gaussian distribution with zero mean and variance $1/\ell$. Note that applying a Gaussian sketch to a vector has an $O(\ell m)$ cost (the explicit storage of the sketch matrix is also $O(\ell m)$), see [14, Chapter 8.3]. When dealing with high dimensional problems, one can also use structured random embeddings, which can reduce the storage and application costs. The most well-used sketches in this case are the subsampled randomized trigonometric transforms (SRTT), subsampled random Fourier transform (SRFT), and the sparse sign embeddings. However, the latter sketches require sufficiently efficient implementations to be faster than a simple Gaussian sketch in practice. For simplicity, in this paper we will only use Gaussian embeddings, but all results can be generalized to the use of other sketching techniques.

One of the most popular uses of sketching is to find approximate solutions of least-squares problems. Suppose we have a tall and skinny matrix $A \in \mathbb{R}^{m \times n}$, where $m \gg n$, then we can define a sketching matrix $S \in \mathbb{R}^{\ell \times m}$, such that $\ell \ll m$ and is assumed to be a small multiple of n . A representation of the sketched matrix $SA \in \mathbb{R}^{\ell \times n}$, of smaller dimension than A , can be observed in Figure 1. The sketch-and-solve method to find an approximate solution to the least-squares problem (2) involves solving the following minimization problem

$$\min_{x \in \mathbb{R}^n} \|S(Ax - b)\|, \quad (5)$$

where S is a sketch matrix, see, e.g. [15], [14, Chapter 10.3]. Note that, when using Gaussian sketching, the solution of (5) is an unbiased estimator of the solution of the original least-squares problem (2) provided that the matrix A has full column rank.

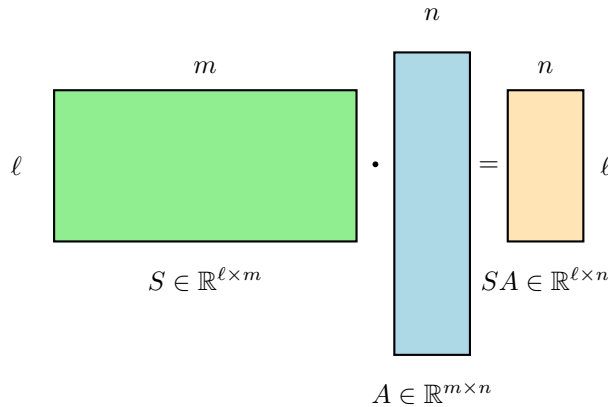


Fig. 1 Schematic representation of the sketching of a matrix A using a sketch S .

The fact that A needs to be tall and skinny seems to be a restrictive property, since a lot of applications do not give rise to systems where the matrices are naturally in this form. However, it has been proposed to use randomized techniques in combination with Krylov methods, where the projections give rise to such tall and skinny matrices. Specifically, for inverse problems, we know that a good approximation of the solution can be found in a Krylov subspace of small dimension involving the right-hand side b , A , and possibly A^T . Thus, as we will describe in Section 3, one can (1) construct a basis for the relevant Krylov subspace(s) and (2) use sketching to solve the projected least-squares problem, since this now involves a tall and skinny matrix even if A was not. The Krylov basis need not be orthogonal, although it should be moderately well-conditioned, so the question is how to construct such a nonorthogonal Krylov basis. Previous approaches have considered using partial reorthogonalization, i.e. truncated (or incomplete) Golub-Kahan or Arnoldi methods, e.g. [16]. However, these require setting an extra hyperparameter, namely the number j of vectors one wants to reorthogonalize against (note that j is usually taken to be $O(1)$). Moreover, inner-products might still be related to algorithmic break-downs in low precision arithmetic due to information loss in the orthogonal projections, see [9] for details. For these reasons, in this paper we propose to use a completely inner-product free construction.

It is worth mentioning that sketching has been used in other contexts as well. Although it is beyond the scope of this paper to give a complete survey of methods, we mention a few examples that relate sketching with iterative Krylov methods. First, the approach of subspace embeddings has been used to sketch the inner products in the Gram-Schmidt orthogonalization procedure [17]. Second, a lot of research has also been done in the use of sketching as preconditioning for iterative methods, for example in the LSNR [18] and Blendenpik [19] algorithms. Both approaches can be more expensive than the sketch-to-solve approach, and target scenarios where high accuracy is required. Since this is typically not the case for inverse problems where the presence of noise and ill-conditioning limit reconstruction accuracy, neither of these paradigms will be addressed in this paper.

In fact, recently, some works have used sketching to do (almost orthogonal) projections onto Krylov subspaces, see, e.g. [20]. In the following section, we give an alternative to construct the basis for the Krylov subspaces that is inherently inner-product free and based on the Hessenberg method with (partial) pivoting. Note that it is well accepted that partial pivoting is stable in practice, even so it is not backwards stable and unstable in the worst case; this is deemed to be very unlikely. In other words, we refer to the following quote attributed to Wilkinson: *“Anyone that unlucky has already been run over by a bus!”*.

3 Inner-product free Krylov subspace methods

Krylov iterative algorithms are a class of very powerful projection methods that make use of Krylov subspaces of the form:

$$\mathcal{K}_k(C, d) = \text{span}\{d, Cd, C^2d, \dots, C^{k-1}d\},$$

for a given matrix C and a vector d . In their most general form, they can be classified by the (Krylov) solution subspace, where a solution at each iteration is sought. The optimality conditions that are imposed determine the solution in that subspace. For orthonormal bases, the optimality conditions are usually given in terms of the orthogonality of the residual with respect to another Krylov subspace.

In this section, we focus on inner-product free Krylov methods, where the first step is to build a nonorthogonal basis for the relevant Krylov subspaces. In Section 3.1 we describe CMRH and LSLU, two inner-product free quasi-minimum residual methods. A key component of these approaches is the (generalized) Hessenberg method used to generate bases for Krylov subspaces without using inner-products and in a practically stable manner. Then, in Section 3.2, we describe our proposed approaches sCMRH and sLSLU, which are inner-product free methods that seek to minimize the residual norm or Tikhonov objective function, where sketching is used to solve the projected problem efficiently.

3.1 CMRH and LSLU: quasi-minimum residual methods

As described in the introduction, the Hessenberg method is an inner-product free approach to generate a basis for $\mathcal{K}_k(A, b)$ [6, 7] where A is a square matrix. That is, after k iterations, we have a unit lower triangular matrix $L_{k+1}^{(s)}$ and an upper Hessenberg matrix $H_{k+1,k}^{(s)}$ that satisfy

$$AL_k^{(s)} = L_{k+1}^{(s)} H_{k+1,k}^{(s)}, \quad (6)$$

where the range of $L_k^{(s)}$ is $\mathcal{K}_k(A, b)$. For rectangular matrices A , the generalized Hessenberg process [9] was established as an inner-product free method to generate bases for both $\mathcal{K}_k(A^T A, A^T b)$ and $\mathcal{K}_k(AA^T, b)$. In this case, the following two relations are updated at each iteration,

$$\begin{aligned} AL_k^{(r)} &= D_{k+1} H_{k+1,k}^{(r)} \\ A^T D_{k+1} &= L_{k+1}^{(r)} W_{k+1}, \end{aligned} \quad (7)$$

where the range of $L_k^{(r)}$ is $\mathcal{K}_k(A^T A, A^T b)$, the range of D_{k+1} is $\mathcal{K}_k(AA^T, b)$ and both matrices are unit lower triangular. Moreover, $H_{k+1,k}^{(r)}$ is upper Hessenberg and W_{k+1} is upper triangular. For the analysis of this method, see [9].

In the previous paragraph, we used the superscript $^{(s)}$ for quantities resulting from applying the Hessenberg method to *square* matrices, and the superscript $^{(r)}$ for quantities resulting from applying the generalized Hessenberg method to *rectangular* matrices. But from now on we will drop the superscript for L_k (and $H_{k+1,k}$), under the general assumption that the range of L_k is a relevant Krylov subspace, and that both matrices are obtained after k iterations of either the Hessenberg or the generalized Hessenberg method.

Finding the minimal residual norm solution in the corresponding Krylov subspace spanned by the columns of L_k (and x_0) corresponds to solving:

$$y_k^{(LS)} = \arg \min_{y \in \mathbb{R}^k} \|AL_k y - b\|, \quad x_k^{(LS)} = L_k y_k^{(LS)} + x_0. \quad (8)$$

However, the columns of L_k (and, if relevant, D_k) are not orthonormal. Therefore, it is not straightforward to use the relations in (6) or (7) to reduce the least-squares problem (8) into a small projected problem. This is different from other standard Krylov methods, like GMRES and LSQR, where the Arnoldi relationship or the Golub-Kahan bidiagonalization can be used to solve (8) efficiently [12, 21]. Note that this is the main drawback of this type of Krylov basis construction. However, recall that the basis vectors are computed in a stable way in practice using (partial) pivoting. Moreover, the approach is inherently inner-product free.

There are Krylov subspace methods that use the relations (6) or (7) to approximate the orthogonal projection (8) by an oblique projection of the residual. For example, the CMRH method for square matrices A [6–8], and the LSLU method for rectangular matrices [9] seek to approximate the least squares solution by computing,

$$x_k = \arg \min_{x \in x_0 + R(L_k)} \|M_{k+1}^\dagger (Ax - b)\|, \quad (9)$$

where $M_{k+1} = L_{k+1}^{(s)}$ for CMRH and $M_{k+1} = D_{k+1}$ for LSLU, and M_{k+1}^\dagger is the Moore-Penrose pseudoinverse of M_{k+1} . The residual norm associated with this solution x_k fulfills the following inequality:

$$\|Ax^{(LS)} - b\| \leq \|Ax_k - b\| \leq \kappa(M_{k+1}) \|Ax^{(LS)} - b\| \quad (10)$$

where $\kappa(\cdot)$ denotes the condition number and from (8), $x^{(LS)}$ is the minimal norm solution in the given Krylov subspace: $\|Ax^{(LS)} - b\| = \min_{x \in x_0 + R(L_k)} \|Ax - b\|$. For more details, see [8] for CMRH and [9] for LSLU.

Note that an interesting interpretation of CMRH and LSLU, which was not noted in the original papers, is that it corresponds to the following approximation of (8),

$$x_k^{(LS)} = L_k y_k^{(LS)} = L_k (M_{k+1} H_{k+1,k})^\dagger b \approx L_k H_{k+1,k}^\dagger M_{k+1}^\dagger b.$$

In other words, an approximate solution for (8) can be obtained in two stages,

$$z_k = \arg \min_{z \in \mathbb{R}^k} \|M_{k+1} z - b\|, \quad (11)$$

$$x_k = L_k (H_{k+1,k}^T H_{k+1,k})^{-1} H_{k+1,k}^T z_k. \quad (12)$$

However, the approximation of the pseudoinverse of the product as $(M_{k+1} H_{k+1,k})^\dagger \approx H_{k+1,k}^\dagger M_{k+1}^\dagger$, is not true in general. Assuming no breakdown, M_{k+1} has full column rank, so the approximation is exact in the case where $H_{k+1,k}$ has full row rank. In the next section, we consider a sketched approximation of $(M_{k+1} H_{k+1,k})^\dagger$.

3.2 sCMRH and sLSLU: sketched inner-product free methods

In this paper, we propose new methods that use the (non-orthogonal) basis vectors for the relevant Krylov subspace, generated with the Hessenberg or the generalized Hessenberg method, and approximately compute the solution of the projected least squares problem using a sketch-and-solve approach. The sketched, projected problem is given by

$$\min_{y \in \mathbb{R}^k} \|S(AL_k y - b)\|, \quad (13)$$

where S is an appropriate sketching matrix. Assuming $x_0 = 0$, the solution at the k th iteration is given by $x_k^{(S)} = L_k y_k^{(S)}$, where $y_k^{(S)}$ is the solution of (13). The crux of our approach lies in the assumption that at any given iteration, the solution $x_k^{(S)}$ will be close to the minimal residual norm solution $x_k^{(LS)}$ with high probability.

Using the subspace embedding property (4) on the residual norm, and recalling that $x^{(LS)}$ is the minimal norm solution in the given Krylov subspace, i.e.,

$$\|Ax^{(LS)} - b\| = \min_{x \in x_0 + R(L_k)} \|Ax - b\|,$$

then one can easily see that

$$\|Ax^{(LS)} - b\| \leq \|Ax_k^{(S)} - b\| \leq \frac{1 + \epsilon}{1 - \epsilon} \|Ax^{(LS)} - b\|. \quad (14)$$

For example, if $S \in \mathbb{R}^{\ell \times m}$ is a Gaussian sketch, (14) holds with a small probability of failure if $\ell \sim m \log(m)/\epsilon^2$ (in practice, this is usually further reduced to $\ell \sim m/\epsilon^2$). Moreover, as noted in [22], ϵ is the subspace embedding constant of the matrix $[A \ b]$ (i.e. appending b to the matrix A). This satisfies $\frac{1+\epsilon}{1-\epsilon} = \kappa_2(SQ^{[A \ b]})$, where $Q^{[A \ b]}$ is the orthogonal matrix obtained doing the QR factorization of $[A \ b]$, and ϵ is usually of the order of 0.5. An accurate mathematical description of the relevant theory can be found in [14, Section 8.7.], and sharper bounds with a different probability of failure can be found in the seminal paper [23].

This means that, in theory one can pick ϵ to be small enough that the solution $x_k^{(S)}$ produced by either sCMRH and sLSLU will have a smaller residual norm than that of the solution x_k obtained using the inner-product free (but not sketched) counterparts. Although this is a very strong motivation of this work, it cannot, however, always be guaranteed in practice.

Moreover, we know that if S is a Gaussian sketch, then the sketch and solve solution to the projected problem is an unbiased estimate for the least-squares solution. Consider the projected problem and the sketched, projected problem,

$$\min_{y \in \mathbb{R}^k} \|AL_k y - b\| \quad \text{and} \quad \min_{y \in \mathbb{R}^k} \|S(AL_k y - b)\|,$$

respectively, where AL_k is a full column rank matrix. Then

$$\mathbb{E}[(SAL_k)^\dagger(Sb)] = (AL_k)^\dagger b$$

where \dagger denotes the Moore-Penrose pseudoinverse. Since L_k is independent of the sketch, we have that $\mathbb{E}[x_k^{(S)}] = \mathbb{E}[L_k(SAL_k)^\dagger(Sb)] = L_k\mathbb{E}[(SAL_k)^\dagger(Sb)] = L_k(AL_k)^\dagger b = x_k^{(LS)}$. In addition, we can further analyze the expected squared residual norm as

$$\begin{aligned}\mathbb{E}[\|AL_k y_k^{(S)} - b\|^2] &= \left(1 + \frac{k}{\ell - k - 1}\right) \min_y \|AL_k y - b\|^2 \\ &= (1 + \varepsilon) \min_y \|AL_k y - b\|^2\end{aligned}$$

when the sketch dimension is $\ell = \frac{k}{\varepsilon} + k + 1$. See [24, 25] and references therein.

Algorithm 1 provides the details for sketched LSLU (sLSLU); the sketched version of CMRH can be straightforwardly generalized. Note that for sLSLU, one sketching matrix is needed $S \in \mathbb{R}^{\ell \times m}$; however, to incorporate Tikhonov regularization, we will need two sketching matrices, $S_1 \in \mathbb{R}^{\ell \times n}$ and $S_2 \in \mathbb{R}^{\ell \times m}$.

As can be observed in Algorithm 1, the generalized Hessenberg method with partial pivoting requires locating the largest absolute value of r_0 , v_0 , and two other vectors at each iteration, which can be costly due to global communications. To avoid this occurrence, a pivoting alternative was proposed in [9] where only a small subset of elements in those vectors is observed, and the pivot is taken to be the element with the largest absolute value from this subset. In practice, this leads to a reduced communication cost and a stable way of building the non-orthogonal basis for the relevant Krylov Subspace methods: in our experiments, we never observed the condition number of the basis to grow significantly large. However, this strategy might still increase the condition number $\kappa(M_{k+1})$ in equation (10), rendering the solutions from LSLU and CMRH less accurate. Therefore, this is a particular case of LSLU and CMRH where the sketched methods have a great potential compared to their non-sketched counterparts. All numerical results will implement this technique for different sample sizes.

From Theorem 2.1 of [9], the authors derived a bound on the difference between the residual norms of solutions computed using LSLU and LSQR. It was shown that if the condition number of \hat{R}_{k+1} , the upper triangular matrix from the QR decomposition of D_{k+1} , does not grow too quickly, then the residual norms associated with the approximate solutions of LSLU and LSQR at each iteration are close to each other. In Section 4, we will compare the residual norm of sLSLU with the residual norms from Theorem 2.1 of [9].

In the next subsection we propose a sketch-and-solve approach to project the Tikhonov problem on a Krylov subspace and approximately compute the solution of the least squares problem (13).

3.3 Extensions for Tikhonov Regularization

Consider the standard Tikhonov regularization problem (3). The LSLU method computes a solution at the k th iteration to the following optimization problem

$$\min_{x \in x_0 + \mathcal{R}(L_k)} \|D_{k+1}^\dagger(b - Ax)\|^2 + \lambda^2 \|L_k^\dagger x\|^2, \quad (15)$$

Algorithm 1 sLSLU

Require: $A, b, x_0, \text{maxiter}, S_1, S_2$

```
1: Define  $t = [1, 2, \dots, m]^T, g = [1, \dots, n]^T$ .
2:  $r_0 = b - Ax_0$ 
3: Determine  $i$  such that  $|r_0(i)| = \|r_0\|_\infty$ 
4:  $\beta = r_0(i); d_1 = r_0/\beta; t(1) \Leftrightarrow t(i)$ 
5:  $v_0 = A^T r_0$ 
6: Determine  $i_2$  such that  $|v_0(i_2)| = \|v_0\|_\infty$ 
7:  $\alpha = v_0(i_2); l_1 = v_0/\alpha; g(1) \Leftrightarrow g(i_2)$ 
8:  $r = A^T d_1; W(1, 1) = r(g(1))$ 
9: for  $k = 1, \dots, \text{maxiter}$  do
10:    $u = A^T d_k$ 
11:    $z_k = S_2 * u$ 
12:   for  $j = 1, \dots, k$  do
13:      $H(j, k) = u(t(j)); u = u - H(j, k)d_j$ 
14:   end for
15:   if  $k < m$  and  $u \neq 0$  then
16:     Determine  $i \in \{k + 1, \dots, m\}$  such that  $|u(t(i))| = \|u(t(k + 1 : m))\|_\infty$ 
17:      $H(k + 1, k) = u(t(i)); d_k = u/H(k + 1, k); t(k + 1) \Leftrightarrow t(i)$ 
18:   else
19:      $H(k + 1, k) = 0;$ 
20:   end if
21:    $q = A^T d_k$ 
22:   for  $j = 1, \dots, k$  do
23:      $W(j, k + 1) = q(g(j)); q = q - W(j, k + 1)l_j$ 
24:   end for
25:   if  $k < n$  and  $q \neq 0$  then
26:     Determine  $i_2 \in \{k + 1, \dots, n\}$  such that  $|q(g(i_2))| = \|q(g(k + 1 : n))\|_\infty$ 
27:      $W(k + 1, k + 1) = u(g(i_2)); l_{k+1} = q/W(k + 1, k + 1); g(k + 1) \Leftrightarrow g(i_2)$ 
28:   else
29:     break
30:   end if
31:   Compute  $y_k$  to be the minimizer of  $\|S_2 r_0 - S_2 A L_k y\|_2^2 = \|S_2 r_0 - Z y\|_2^2$ 
32:    $x_k = x_0 + L_k y_k$ 
33: end for
```

where similar to LSLU, the residual norm is replaced by a semi-norm, and the regularization term also includes a semi-norm. This is equivalent to solving

$$y_{\lambda,k} = \arg \min_{y \in \mathbb{R}^k} \|\beta e_1 - H_{k+1,k} y\|^2 + \lambda^2 \|y\|^2, \quad (16)$$

where β is selected using the following sample strategy in [9]: select a small random sample of entries from r_0, v_0, u, q and choose the largest value (in magnitude) in that sample. Similarly, one can use a sketch-and-solve approach to project the Tikhonov problem on a Krylov subspace and approximately compute the solution of the least

squares problem using the following expression:

$$\min_{y \in \mathbb{R}^k} \|S_2(AL_k y - b)\| + \lambda^2 \|S_1(L_k y)\|^2, \quad (17)$$

where S_1 and S_2 are appropriate sketching matrices. Similar to LSQR and LSLU, the authors of [9] derived a bound on the difference between the residual norms of solutions computed using LSLU and LSQR for the Tikhonov problem. It was shown that if the condition number of \bar{D}_{k+1} from the block matrix

$$\bar{D}_{k+1} = \begin{bmatrix} D_{k+1} & 0 \\ 0 & L_k \end{bmatrix} \quad (18)$$

does not grow too quickly, then the residual norms associated to the solution of LSLU for the Tikhonov problem is close to the residual norm of the solution obtained with LSQR for the Tikhonov problem (See Theorem 3.1 of [9]). To display behavior of sLSLU with Tikhonov regularization, we will plot the associated residual norm against the residuals norms denoted in Theorem 3.1 of [9] (See Section 4). An implementation of sLSLU with Tikhonov regularization is provided in Algorithm 2, which corresponds to Algorithm 1 if $\lambda = 0$. Note that for all numerical results, we select a fixed regularization parameter. The correspondent implementation of sCMRH with Tikhonov regularization can be easily generalized.

Algorithm 2 sLSLU with Tikhonov Regularization

Require: $A, b, x_0, \text{maxiter}, S_1, S_2, \lambda$

```
1: Define  $t = [1, 2, \dots, m]^T, g = [1, \dots, n]^T$ .
2:  $r_0 = b - Ax_0$ 
3: Determine  $i$  such that  $|r_0(i)| = \|r_0\|_\infty$ 
4:  $\beta = r_0(i); d_1 = r_0/\beta; t(1) \Leftrightarrow t(i)$ 
5:  $v_0 = A^T r_0$ 
6: Determine  $i_2$  such that  $|v_0(i_2)| = \|v_0\|_\infty$ 
7:  $\alpha = v_0(i_2); l_1 = v_0/\alpha; g(1) \Leftrightarrow g(i_2)$ 
8:  $r = A^T d_1; f_1 = S_1 * r; W(1, 1) = r(g(1))$ 
9: for  $k = 1, \dots, \text{maxiter}$  do
10:    $u = A^T d_k$ 
11:    $z_k = S_2 * u$ 
12:   for  $j = 1, \dots, k$  do
13:      $H(j, k) = u(t(j)); u = u - H(j, k)d_j$ 
14:   end for
15:   if  $k < m$  and  $u \neq 0$  then
16:     Determine  $i \in \{k + 1, \dots, m\}$  such that  $|u(t(i))| = \|u(t(k + 1 : m))\|_\infty$ 
17:      $H(k + 1, k) = u(t(i)); d_k = u/H(k + 1, k); t(k + 1) \Leftrightarrow t(i)$ 
18:   else
19:      $H(k + 1, k) = 0;$ 
20:   end if
21:    $q = A^T d_k$ 
22:    $f_{k+1} = S_1 q$ 
23:   for  $j = 1, \dots, k$  do
24:      $W(j, k + 1) = q(g(j)); q = q - W(j, k + 1)l_j$ 
25:   end for
26:   if  $k < n$  and  $q \neq 0$  then
27:     Determine  $i_2 \in \{k + 1, \dots, n\}$  such that  $|q(g(i_2))| = \|q(g(k + 1 : n))\|_\infty$ 
28:      $W(k + 1, k + 1) = q(g(i_2)); l_{k+1} = q/W(k + 1, k + 1); g(k + 1) \Leftrightarrow g(i_2)$ 
29:   else
30:     break
31:   end if
32:   Compute  $y_{\lambda_k, k}$  to be the minimizer of  $\|S_2 r_0 - S_2 A L_k y\|_2^2 + \lambda^2 \|S_1 L_k y\|$ 
33:    $x_k = x_0 + L_k y_{\lambda_k, k}$ 
34: end for
```

4 Numerical Results

In this section, we illustrate the effectiveness of sketched inner-product-free Krylov methods: sketched CMRH (sCMRH) and sketched LSLU (sLSLU) in comparison to their non-sketched counterparts CMRH and LSLU [9], and the classical GMRES and LSQR. We utilize three different test problems: a deblurring problem, a neutron tomography simulation from the IR Tools package [26], and an example with real data consisting of two open access datasets from the Finnish Inverse Problems

Society [27, 28]. Moreover, for Tikhonov regularization with fixed λ , we provide numerical results for sLSLU, LSLU, and LSQR for some of these test problems. Note that each sketch matrix has the following dimensions: $S_1 \in \mathbb{R}^{\ell \times n}$, $S_2 \in \mathbb{R}^{\ell \times m}$ where $\ell = 10 * (\text{max iteration} + 1)$.

4.1 Deblurring problem

The first experiment consists of a deblurring experiment, where the aim is to reconstruct MATLAB’s test image ‘cameraman’ of size 256×256 pixels, which was corrupted by motion blur and additive Gaussian noise. The forward model was simulated using IR Tools [26], and noise was added so that the observation contained a 1% noise level.

Since this is a square problem, we compare sCMRH to CMRH and GMRES. The relative reconstruction error norm and residual norms per iteration are displayed in Figure 2. We observe that the curves corresponding to sCMRH closely resembles that of GMRES, as dictated by the theory, while the residual norms for CMRH deviate as the iterations proceed. This can also be observed in the relative error norms. Thus, sCMRH produces solutions that more closely resemble GMRES solutions, but without the need for inner-product computations. The reconstructed images are shown in Figure 3.

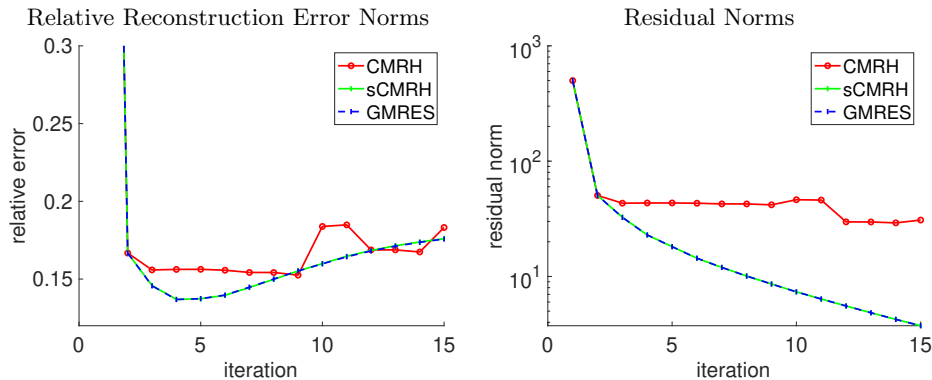


Fig. 2 Relative reconstruction error norms (left) and residual norms (right). In this case, sketched CMRH uses the pivots dictated by the maximum absolute value from a set of randomly sampled coefficients (5).

4.2 Neutron tomography simulation

Neutron imaging is a tomography technique based on gamma-rays that allows us to inspect the interior of dense or metallic objects. This is because, contrary to X-ray tomography, the absorption of neutrons is higher in ‘light’ elements and lower in metallic elements. See, for example, the interior of a padlock in [29]. Note that, mathematically, this CT modality has the same mathematical model as X-ray tomography, but using different absorption coefficients for each material. Since most datasets for

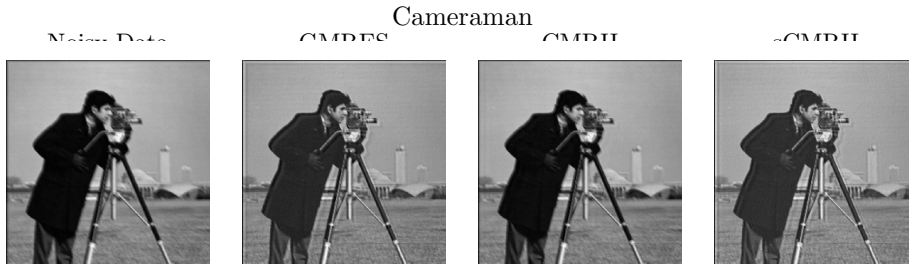


Fig. 3 Measured noisy data, and reconstructed images using GMRES, CMRH, and sCMRH.

this type of tomography are proprietary, in this example, we use MATLAB’s built-in demo image ‘circuit.tiff’, which has similar structure to neutron tomography examples.

The sketched LSLU (sLSLU) algorithm implements the pivoting alternative from [9]. The sample size to approximate the infinity norm contains 25 entries. Note that varying the sample size does not appear to drastically change the numerical results. In Figure 4, we provide the relative reconstruction error norms per iteration of sLSLU. Results for LSQR and LSLU are provided for comparison. We observe that sLSLU performs better than LSLU and similar to LSQR, especially in the earlier iterations. Provided we implement a “good” stopping criteria, we can compute an approximation that is of comparable quality to that produced with LSQR; while avoiding inner-products.

The residual norms are also plotted for comparison (see right plot in Figure 4). In Figure 4, we find that residual norms for sLSLU closely follow the lower bound, which corresponds to residual norms for LSQR. Similar to the relative error plot, we find that the behavior of sLSLU aligns with LSQR, and the reconstructions are provided in Figure 5.

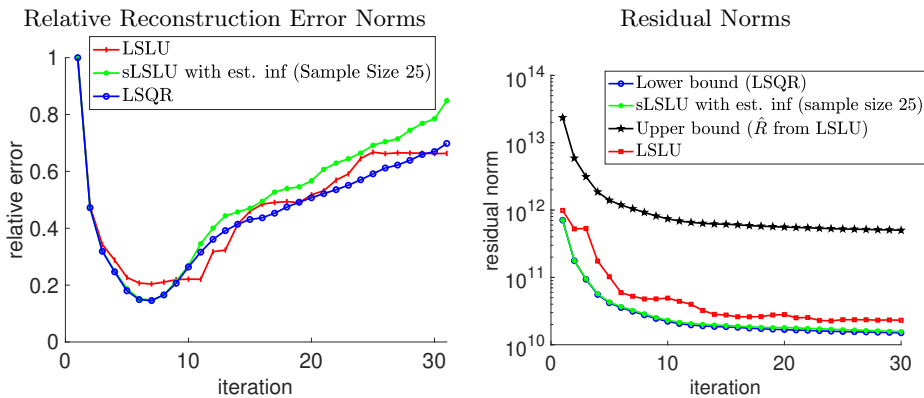


Fig. 4 Relative reconstruction error norms (left) and residual norms (right). In this case, sketched LSLU uses the pivots dictated by the maximum absolute value from a set of randomly sampled coefficients (25).

Neutron Tomography Simulation

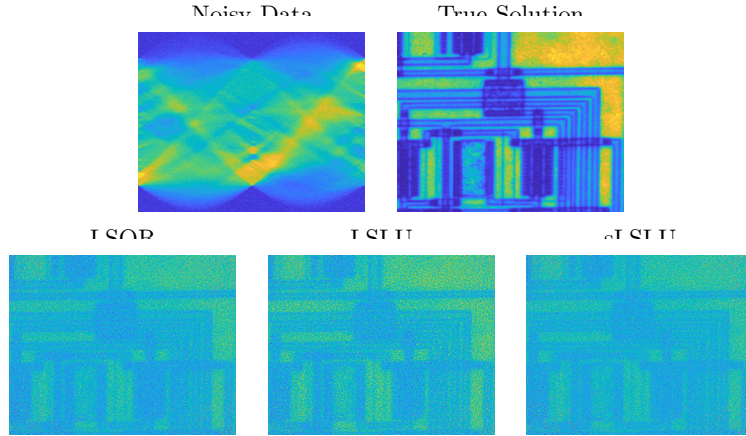


Fig. 5 Measured noisy data, true solution, and reconstructed images from LSQR, LSLU, and sLSLU. The image proportions are accurate but, to aid visualization, the relative size between images is not.

Next we consider the performance of sLSLU for the Tikhonov problem. We fix $\lambda = 26$, and we plot the residual norm of sLSLU compared to LSLU and LSQR in Figure 6. We also provide the relative reconstruction error norms per iteration. We observe that the inclusion of the regularization term stabilizes the semi-convergence for all methods. For the Tikhonov problem, sLSLU mirrors the behavior of LSQR on the Tikhonov problem. An adaptive approach to find a “good” regularization parameter during the iterations is a topic of future work. Image reconstructions corresponding to 30 iterations are provided in Figure 7.

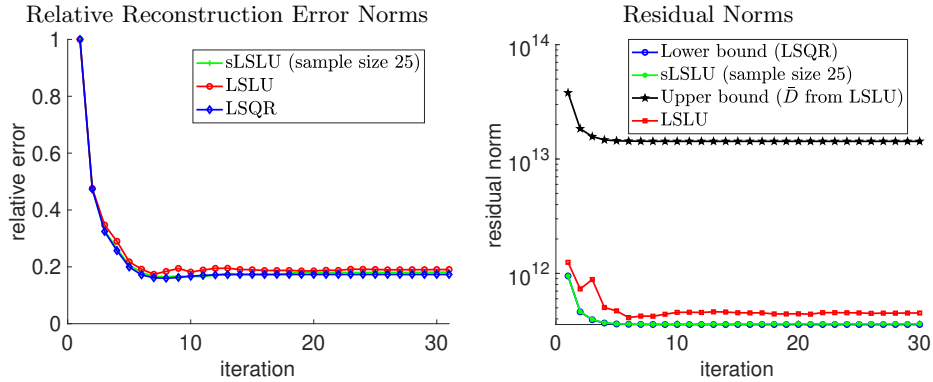


Fig. 6 Relative reconstruction error norms (left) and residual norms (right). In this case, sketched LSLU with Tik. Reg. uses pivots dictated by the maximum absolute value from a set of randomly sampled coefficients (25).

Neutron Tomography Simulation

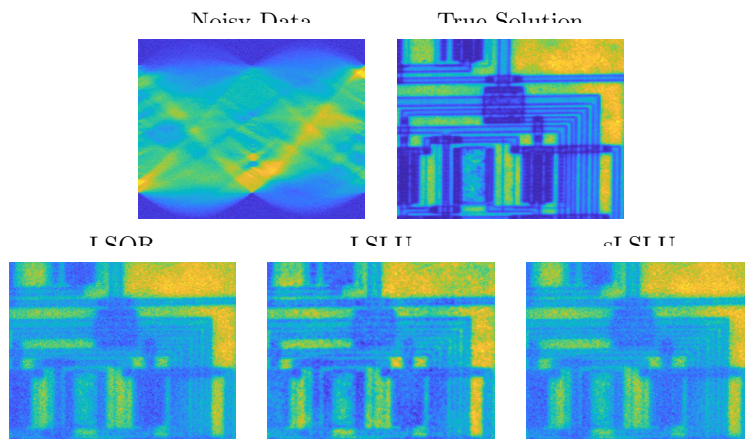


Fig. 7 Measured noisy data, true solution, and reconstructed LSQR, LSLU, and sLSLU for solving the Tikhonov problem. The image proportions are accurate but, to aid visualization, the relative size between images is not.

4.3 Real data examples

The Finnish Inverse Problems Society has provided the following open access datasets: a tomographic x-ray of carved cheese and a walnut. Both datasets consist of X-ray sinograms where each sinogram is obtained by fan-beam projection. The observed data for the carved cheese dataset containing 360 projections and the walnut dataset containing 120 projections are provided in Figures 9 and 10 respectively. For these problems, there is no true image, so we rely on residual norms per iteration to compare algorithms.

To illustrate the behavior of the residual norms for sLSLU, LSLU, and LSQR as well as the bounds in Theorem 2.1 of [9], we plot in Figure 8 the residual norms per iteration for the carved cheese and walnut datasets. The samples size to approximate the infinity norm contains 25 entries. For both datasets, we observe that the residual norms for sLSLU and LSQR remain close together, with the residual norms for LSLU being a bit larger. Therefore, we may expect that the approximate solutions from sLSLU should mirror those from LSQR. This is verified in Figure 9 and Figure 10, where the reconstructed images using LSQR, LSLU, and sLSLU are provided. All reconstructions correspond to iteration 30.

Finally, we consider sLSLU with Tikhonov regularization for these examples, where we plot the the residual norm of sLSLU with Tikhonov regularization in Figure 11. We fix $\lambda = 1$ for both problems. Similar to the nonregularized problems, the residual norms for sLSLU closely follow the lower bound, which corresponds to residual norms for LSQR. Thus, we may expect that provided we have a “good” estimate for the regularization parameter, sLSLU with Tikhonov regularization will produce a better approximation of the solution than LSLU on the Tikhonov problem. We also provide reconstructed images for both datasets in Figure 12 and Figure 13.

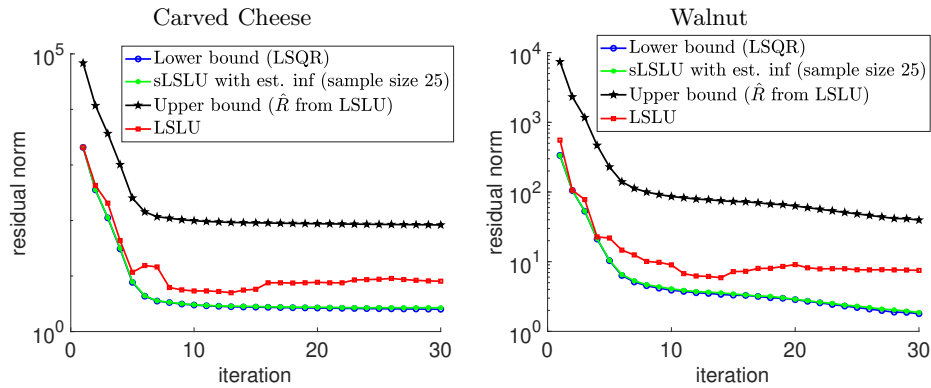


Fig. 8 Residual norms per iteration for sLSLU and LSLU, as well as corresponding bounds from Theorem 2.1 of [9]. Note that the lower bound corresponds to LSQR residual norms.

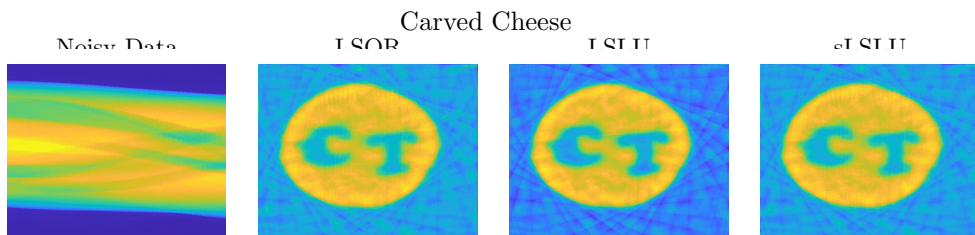


Fig. 9 Measured noisy data, and reconstructed images from LSQR, LSLU, and sLSLU. The image proportions are accurate but, to aid visualization, the relative size between images is not.

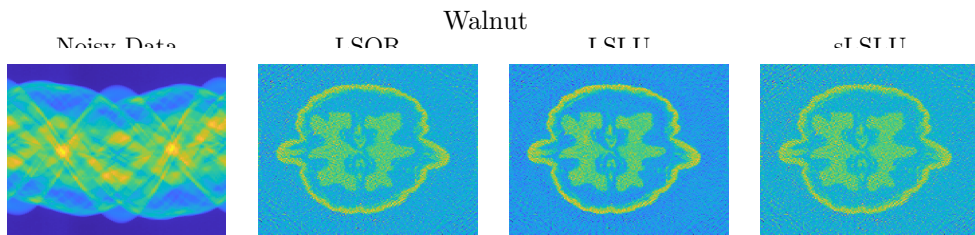


Fig. 10 Measured noisy data, and reconstructed images from LSQR, LSLU, and sLSLU. The image proportions are accurate but, to aid visualization, the relative size between images is not.

5 Conclusions

In this paper, we introduce two new inner-product free Krylov methods, sCMRH and sLSLU, that incorporate randomization techniques for solving large-scale linear inverse problems. Both methods are based on the Hessenberg method with partial pivoting for building bases that span Krylov subspaces, and hence do not require inner-product computations (e.g., orthogonalizations). Also, both sCMRH and sLSLU exploit randomized sketching to solving the projected problems, thereby producing solutions with a smaller residual norm compared to existing inner-product free Krylov methods. Numerical experiments show that the performance of sCMRH is comparable to

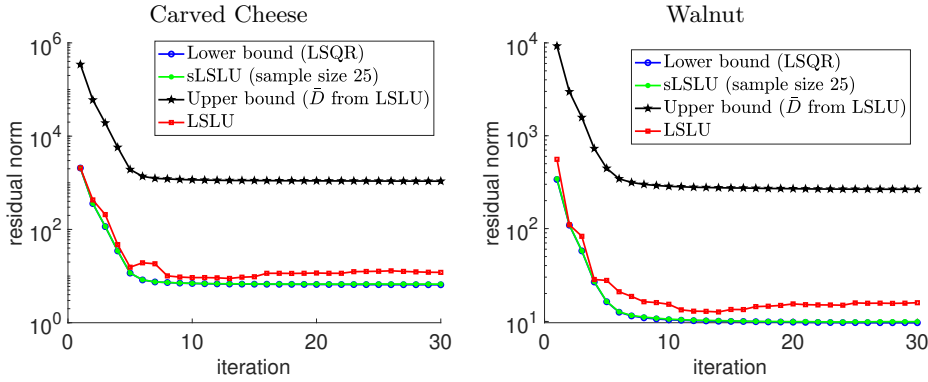


Fig. 11 Residual norms per iteration for the Tikhonov problem correspond to sLSLU, LSLU, as well as corresponding bounds from Theorem 3.1 of [9]. Note that the lower bound corresponds to LSQR. The regularization parameter $\lambda = 1$.

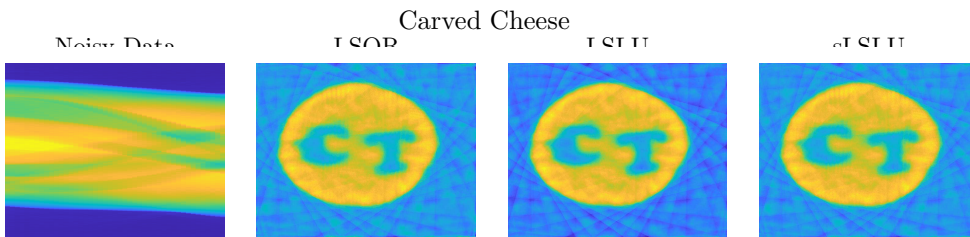


Fig. 12 Measured noisy data, and Tikhonov reconstructions for LSQR, LSLU, and sLSLU. The image proportions are accurate but, to aid visualization, the relative size between images is not.

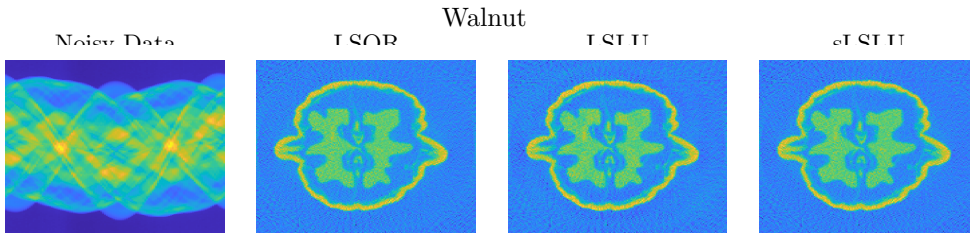


Fig. 13 Measured noisy data, and Tikhonov reconstructions for LSQR, LSLU, and sLSLU. The image proportions are accurate but, to aid visualization, the relative size between images is not.

that of GMRES and the performance of sLSLU is comparable to that of LSQR. Moreover, sCMRH and sLSLU have smaller residual norm solutions, compared to CMRH and LSLU respectively. The sketched Krylov methods can be adapted to incorporate Tikhonov regularization provided that an appropriate regularization parameter is selected. Since sCMRH and sLSLU are all inner-product free, they may be useful in solving problems with mixed-precision and parallel computing, which is a topic of future work.

Acknowledgements. We would like to acknowledge Ethan Epperly’s blog, which provided us with nice expositions: <https://www.ethanepperly.com/index.php/blog>

Funding. This work was partially funded by the U.S. National Science Foundation, under grants DMS-2038118, DMS-2411197 and DMS-2208294. Any opinions, finding, and conclusions or recommendations expressed in this material are those of the author(s) and do not necessarily reflect the views of the National Science Foundation.

References

- [1] Chung, J., Knepper, S., Nagy, J.G.: Large-scale inverse problems in imaging. In: Scherzer, O. (ed.) *Handbook of Mathematical Methods in Imaging*, pp. 47–90. Springer, New York, NY (2015). https://doi.org/10.1007/978-1-4939-0790-8_2
- [2] Hansen, P.C.: *Discrete Inverse Problems: Insight and Algorithms*. SIAM, Philadelphia (2010)
- [3] Vogel, C.R.: *Computational Methods for Inverse Problems*. SIAM, Philadelphia (2002)
- [4] Zhdanov, M.: *Geophysical Inverse Theory and Regularization Problems* vol. 36. Elsevier, New York (2002)
- [5] Faddeev, D.K., Faddeeva, V.N.: *Computational Methods of Linear Algebra*. Freeman, San Francisco and London (1963). Translated by R. C. Williams
- [6] Sadok, H.: CMRH: A new method for solving nonsymmetric linear systems based on the Hessenberg reduction algorithm. *Numer. Algor.* **20**, 303–321 (1999)
- [7] Sadok, H., Szyld, D.B.: A new look at CMRH and its relation to GMRES. *BIT Numerical Mathematics* **52**, 485–501 (2012) <https://doi.org/10.1007/s10543-011-0365-x>
- [8] Brown, A.N., Sabaté Landman, M., Nagy, J.G.: H-CMRH: An inner product free hybrid Krylov method for large-scale inverse problems. *SIAM Journal on Matrix Analysis and Applications* **46**(1), 232–255 (2025) <https://doi.org/10.1137/24M1634874>
- [9] Brown, A.N., Chung, J., Nagy, J.G., Sabaté Landman, M.: Inner product free Krylov methods for large-scale inverse problems (2024). <https://arxiv.org/abs/2409.05239>
- [10] Paige, C.C., Saunders, M.A.: LSQR: An algorithm for sparse linear equations and sparse least squares. *ACM Transactions on Mathematical Software (TOMS)* **8**(1), 43–71 (1982)

- [11] Paige, C.C., Saunders, M.A.: Algorithm 583: LSQR: Sparse linear equations and least squares problems. *ACM Transactions on Mathematical Software (TOMS)* **8**(2), 195–209 (1982)
- [12] Saad, Y.: *Iterative Methods for Sparse Linear Systems*, 2nd edn. SIAM, Philadelphia (2003)
- [13] Calvetti, D., Somersalo, E.: *An Introduction to Bayesian Scientific Computing: Ten Lectures on Subjective Computing* vol. 2. Springer, New York (2007)
- [14] Martinsson, P.-G., Tropp, J.A.: Randomized numerical linear algebra: Foundations and algorithms. *Acta Numerica* **29**, 403–572 (2020) <https://doi.org/10.1017/S0962492920000021>
- [15] Sarlos, T.: Improved approximation algorithms for large matrices via random projections. In: 2006 47th Annual IEEE Symposium on Foundations of Computer Science (FOCS'06), pp. 143–152 (2006). <https://doi.org/10.1109/FOCS.2006.37>
- [16] Güttel, S., Schweitzer, M.: Randomized sketching for Krylov approximations of large-scale matrix functions. *SIAM Journal on Matrix Analysis and Applications* **44**(3), 1073–1095 (2023) <https://doi.org/10.1137/22M1518062>
- [17] Balabanov, O., Grigori, L.: Randomized Gram–Schmidt process with application to GMRES. *SIAM Journal on Scientific Computing* **44**(3), 1450–1474 (2022) <https://doi.org/10.1137/20M138870X> <https://doi.org/10.1137/20M138870X>
- [18] Meng, X., Saunders, M.A., Mahoney, M.W.: LSRN: A parallel iterative solver for strongly over- or underdetermined systems. *SIAM Journal on Scientific Computing* **36**(2), 95–118 (2014) <https://doi.org/10.1137/120866580>
- [19] Avron, H., Maymouk, P., Toledo, S.: Blendepik: Supercharging LAPACK’s least-squares solver. *SIAM Journal on Scientific Computing* **32**(3), 1217–1236 (2010) <https://doi.org/10.1137/090767911>
- [20] Nakatsukasa, Y., Tropp, J.A.: Fast and accurate randomized algorithms for linear systems and eigenvalue problems. *SIAM Journal on Matrix Analysis and Applications* **45**(2), 1183–1214 (2024) <https://doi.org/10.1137/23M1565413> <https://doi.org/10.1137/23M1565413>
- [21] Golub, G.H., Van Loan, C.V.: *Matrix Computations*, 4th edn. John Hopkins University Press, Baltimore (2013)
- [22] Meier, M., Nakatsukasa, Y., Townsend, A., Webb, M.: Are sketch-and-precondition least squares solvers numerically stable? *SIAM Journal on Matrix Analysis and Applications* **45**(2), 905–929 (2024) <https://doi.org/10.1137/23M1551973>

- [23] Sarlos, T.: Improved approximation algorithms for large matrices via random projections. In: 2006 47th Annual IEEE Symposium on Foundations of Computer Science (FOCS'06), pp. 143–152 (2006). <https://doi.org/10.1109/FOCS.2006.37>
- [24] Dereziński, M., Mahoney, M.W.: Recent and upcoming developments in randomized numerical linear algebra for machine learning. In: Proceedings of the 30th ACM SIGKDD Conference on Knowledge Discovery and Data Mining, pp. 6470–6479 (2024)
- [25] Drineas, P., Mahoney, M.W., Muthukrishnan, S., Sarlós, T.: Faster least squares approximation. *Numerische mathematik* **117**(2), 219–249 (2011)
- [26] Gazzola, S., Hansen, P.C., Nagy, J.G.: IR Tools: a MATLAB package of iterative regularization methods and large-scale test problems. *Numer. Algorithms* **81**(3), 773–811 (2019) <https://doi.org/10.1007/s11075-018-0570-7>
- [27] Bubba, T.A., Juvonen, M., Lehtonen, J., März, M., Meaney, A., Purisha, Z., Siltanen, S.: Tomographic x-ray data of carved cheese. arXiv preprint arXiv:1705.05732 (2017)
- [28] Hämäläinen, K., Harhanen, L., Kallonen, A., Kujanpää, A., Niemi, E., Siltanen, S.: Tomographic x-ray data of a walnut. arXiv preprint arXiv:1502.04064 (2015)
- [29] Biguri, A., Sadakane, T., Lindroos, R., Liu, Y., Landman, M.S., Du, Y., Lohvithee, M., Kaser, S., Hatamikia, S., Bryll, R., Valat, E., Wonglee, S., Blumensath, T., Schönlieb, C.-B.: Tigre v3: Efficient and easy to use iterative computed tomographic reconstruction toolbox for real datasets. ArXiv preprint (2024) [arXiv:2412.10129](https://arxiv.org/abs/2412.10129)